

# Physicochemical Study of Catalysts for the Oxidative Dehydrogenation of Isobutane: Cobalt, Nickel, and Manganese Molybdates

Yu. A. Agafonov, N. V. Nekrasov, N. A. Gaidai, M. A. Botavina,  
P. E. Davydov, and A. L. Lapidus

Zelinskii Institute of Organic Chemistry, Russian Academy of Sciences, Moscow, 119991 Russia

e-mail: gaidai@server.ioc.ac.ru

Received April 12, 2007; in final form, May 12, 2008

**Abstract**—Temperature-programmed desorption and IR spectroscopic studies of the physicochemical properties of cobalt, nickel, and manganese molybdates are reported. These properties are correlated with the catalytic properties of the molybdates in the oxidative dehydrogenation of isobutane with atmospheric oxygen. It is demonstrated by an analysis of the IR spectra of the molybdates that the isobutene yield grows as the proportion of tetrahedrally coordinated molybdenum in the catalyst structure increases in isobutane dehydrogenation.  $\text{NiMoO}_4$  has the highest surface concentration of strong acid sites, and it binds adsorbed isobutene more strongly than the other catalysts.

**DOI:** 10.1134/S0023158409040156

Because of the necessity of raising the efficiency of natural gas conversion and because of the steadily increasing world demand for light olefins, great attention in recent years has been focused on the oxidative dehydrogenation of light paraffins. The oxidative dehydrogenation reactions of light paraffins in the presence of oxygen are usually accompanied by hydrocarbon cracking and deep oxidation. This makes it necessary to carry out a comprehensive study of the oxidative dehydrogenation mechanism. It is particularly significant to see whether there is a correlation between the nature and surface properties of the catalyst and its oxidative dehydrogenation activity.

Here, we report the physicochemical properties of catalysts based on Co, Ni, and Mn molybdates. This work continues the series of our mechanistic studies of the oxidative dehydrogenation of isobutane on these catalytic systems in the presence of atmospheric oxygen [1, 2].

Obviously, the key factor determining the difference between the catalytic activities of the catalysts examined is the nature of the Co, Ni, and Mn ions, which can be directly involved in some steps of the catalytic process and can have an effect on the properties of the active molybdate surface as a whole. It was demonstrated that it is the divalent cations of the molybdates that play the most important role in olefin adsorption [3]. The  $\text{Co}^{2+}$  and  $\text{Ni}^{2+}$  ions form much more stable complexes than the  $\text{Mn}^{2+}$  ion [4].

For metal molybdates, there are two structure types differing in oxygen coordination around the molybdenum atom. Nickel molybdate exists as an  $\alpha$ -phase, in

which the molybdenum atom is octahedrally coordinated, and as a  $\beta$ -phase, in which molybdenum is tetrahedrally coordinated [5]. Phase composition studies demonstrated that, upon heating,  $\alpha\text{-NiMoO}_4$  turns entirely into the  $\beta$ -phase only above  $760^\circ\text{C}$ . Between  $625$  and  $760^\circ\text{C}$ , these phases coexist. When being cooled, the  $\beta$ -phase is stable down to  $250^\circ\text{C}$  [6]. Cobalt molybdate also forms  $\alpha$ - and  $\beta$ -phases with octahedrally and tetrahedrally coordinated molybdenum, respectively. The phase transition temperature in this system is  $673 \pm 10^\circ\text{C}$  [7]. Unlike  $\beta\text{-NiMoO}_4$ ,  $\beta\text{-CoMoO}_4$  is stable at room temperature. Manganese molybdate has a single stable phase, in which the molybdenum atom is in a distorted tetrahedral environment [8].

Molybdates with octahedrally and tetrahedrally coordinated molybdenum have different molecular orbital structures. The orbitals of the former can be involved in  $\sigma$ -donor and  $\pi$ -dative interactions; the orbitals of the latter, only in  $\sigma$ -donor interactions. It is likely that “octahedral” molybdates bind olefins more strongly than “tetrahedral” molybdates. It is to the difference between the coordination polyhedra of molybdenum in  $\alpha$ - and  $\beta\text{-CoMoO}_4$  that Zakharov et al. [9] attribute the difference between the acrolein adsorption properties of these phases.

The stronger the adsorption of the unsaturated hydrocarbon and the higher the acidity of the catalyst, the higher the probability of the subsequent oxidative dehydrogenation of the olefin and, accordingly, the higher the selectivity with respect to the oxidative dehydrogenation products. The lower selectivity of the

Mo- and Mg-containing catalysts for the oxidative dehydrogenation of propane is due to the higher surface concentration of medium-strength and strong acid sites, primarily Lewis sites [10, 11].

Although the oxidative dehydrogenation of isobutane on various molybdates is a redox process [1, 2], the acidity of the catalyst can be a significant factor in the occurrence of undesired processes, such as the cracking and deep oxidation of hydrocarbons, including olefins.

The purpose of this work is to correlate the structure and acid properties of catalysts based on Co, Ni, and Mn molybdates with their efficiency in the oxidative dehydrogenation of isobutane.

## EXPERIMENTAL

### *Catalyst Preparation*

Cobalt, nickel, and manganese molybdates were synthesized by coprecipitation from aqueous solutions of the respective metal nitrates and ammonium molybdate as described in [12].<sup>1</sup> The cobalt-containing sample was obtained using a 5% stoichiometric excess of ammonium molybdate.

### *IR Spectroscopy*

IR spectra were recorded on a Nicolet Protégé 460 spectrophotometer. Samples for the study of the vibrational spectrum of the molybdate lattice were prepared in the following two ways:

(1) pelletization of a molybdate (~0.5%) with crystalline KBr;

(2) deposition of a catalyst from an aqueous suspension onto the surface of a silicon wafer followed by high-temperature treatment.

The transmission spectra of these samples were recorded.

Isobutane adsorption was studied on powder catalysts by diffuse reflectance spectroscopy. The samples were placed in the removable vacuum cell of a Schlenk-type glass setup equipped with a diffusion pump. Isobutane adsorption and spectroscopy were carried out at room temperature.

### *Temperature-Programmed Desorption (TPD)*

Samples to be characterized by TPD (0.5 cm<sup>3</sup>, particle size of 0.25–0.5 mm) were placed in a U-shaped steel reactor and were heat-treated at 400°C in flowing helium for 1 h. For ammonia adsorption, 2.9-ml portions of NH<sub>3</sub> were introduced into the helium flow

<sup>1</sup> The CoMoO<sub>4</sub>, NiMoO<sub>4</sub>, and MnMoO<sub>4</sub> samples were provided by V. Corberan (Instituto de Catálisis y petroquímica, CSIC, Madrid, Spain), M. Portela (CRECAT, Instituto Superior Técnico, Lisbon, Portugal), and F. Trifiro (Università di Bologna, Italy), respectively. We are deeply grateful to these researchers for their help.

until the sample was saturated. The gas detector was a thermal-conductivity detector connected to a computer. The ammonia-saturated sample was purged with flowing helium at room temperature for 30 min. Ammonia TPD was performed in the same helium flow by raising the temperature from 20 to 700°C at a rate of 0.33 K/s. The helium flow rate was maintained at 30 ml/min. TPD spectra were deconvolved into separate peaks using the Origin program to reach a correlation coefficient of  $R > 0.995$ . The TPD profile could be affected by the desorption of the substances that stayed in the molybdate sample after thermal pretreatment and by the release of structural oxygen at high temperature (>500°C). In order to take into account these effects, samples not treated with ammonia were subjected to temperature-programmed heating under the same conditions as were used in NH<sub>3</sub> TPD. The NH<sub>3</sub> TPD profiles presented here were obtained by subtracting the temperature-programmed heating curve from the observed TPD spectrum.

Below 400°C, ammonia is desorbed from Brønsted acid sites of metal oxide catalysts [10, 11]. At higher temperatures, ammonia is likely desorbed from Lewis acid and reversible chemisorption sites.

## RESULTS AND DISCUSSION

### *Structures of Co, Ni, and Mn Molybdates*

In order to reveal the structural differences between the molybdates and determine the factors in their catalytic activity in the oxidative dehydrogenation of isobutane, we carried out IR spectroscopic studies of the vibrations in the 500–1100 cm<sup>-1</sup> range. The spectra of the air-dry initial samples are shown in Fig. 1.

The absorption band at 996 cm<sup>-1</sup> is observed for molybdates containing small amounts of MoO<sub>3</sub> (<10 wt %) [13], so its presence in the spectrum of Co<sub>0.95</sub>MoO<sub>4</sub> is quite natural. The bands in the 700–1000 cm<sup>-1</sup> range are due to the various vibrations of the Mo–O bond. It was demonstrated that the vibrations of the Mo<sup>6+</sup>=O bond are manifested as an absorption band at 1010 cm<sup>-1</sup>, which can be shifted to 990 cm<sup>-1</sup> in the presence of a water ligand, and the vibrations of the Mo<sup>5+</sup>=O bond give rise to a band at 970 cm<sup>-1</sup> [14]. As is clear from Fig. 1, the band at 960–970 cm<sup>-1</sup> is present in the spectra of all systems. However, it appears as a clear-cut separate peak only in the spectrum of nickel molybdate. In the spectra of the other molybdates, it is a shoulder of the main peak (which occurs at 944, 939, and 946 cm<sup>-1</sup> in the spectra of MnMoO<sub>4</sub>, NiMoO<sub>4</sub>, and CoMoO<sub>4</sub>, respectively). Dury et al. [15], who studied the NiMoO<sub>4</sub> catalyst, assigned the absorption band near 940 cm<sup>-1</sup> to the molybdate phase for the reason that this band is not observed for MoO<sub>3</sub> or NiO. Mazzocchia et al. [5] believe that the molybdates with octahedrally coordinated molybdenum are characterized by a band at 945 cm<sup>-1</sup>. However, this belief is inconsistent with the

occurrence of a strong absorption band at  $944\text{ cm}^{-1}$  in the spectrum of manganese molybdate, in which molybdenum is tetrahedrally coordinated [16]. The similar band at  $939\text{ cm}^{-1}$  in the spectrum of nickel molybdate is less well defined than the same band in the spectra of the other molybdates. At the same time, the above-mentioned band at  $990\text{ cm}^{-1}$  shows itself (as a shoulder) only in the spectrum of nickel molybdate. In general, the bands corresponding to the  $\text{Mo}=\text{O}$  bond vibrations are best defined in the spectrum of nickel molybdate, while the characteristic absorption band of the molybdate phase is least pronounced in this spectrum.

According to earlier reports [6, 15, 17, 18], the absorption bands between  $700$  and  $900\text{ cm}^{-1}$  in the spectra of molybdates are due to vibrations of the ordinary bond  $\text{Mo}-\text{O}$ . At the same time, the  $\text{O}-\text{O}$  vibrations of the peroxide ion  $\text{O}_2^{2-}$  manifest themselves in the  $800$ – $900\text{ cm}^{-1}$  range [3, 19]. The Raman spectra of barium-promoted  $\alpha$ - $\text{NiMoO}_4$  samples show bands at  $891$  and  $837\text{ cm}^{-1}$ , which are due to the  $\text{O}-\text{O}$  bond in the peroxide ion. For this reason, the  $815$  and  $875\text{ cm}^{-1}$  bands in the IR absorption spectra of these samples were also assigned [6] to the vibrations of this bond. The  $\beta$ -phases of  $\text{CoMoO}_4$  and  $\text{NiMoO}_4$  are characterized by two absorption bands in the  $780$ – $880\text{ cm}^{-1}$  range [5].

The spectrum of manganese molybdate (Fig. 1) exhibits a number of intense bands between  $700$  and  $900\text{ cm}^{-1}$ , which are much weaker in the spectrum of  $\text{Co}_{0.95}\text{MoO}_4$  and particularly in the spectrum of  $\text{NiMoO}_4$ .

Examination of the IR spectra of various molybdates [20] demonstrated that the presence of absorption bands in the  $600$ – $700\text{ cm}^{-1}$  range is evidence of the formation of molybdate hydroxo complexes. The spectra of cobalt and nickel molybdates show well-defined absorption bands at  $661$  and  $651\text{ cm}^{-1}$ , respectively. It is likely that the hydroxyl concentration on the cobalt and nickel molybdate surfaces is much higher than the hydroxyl concentration on the manganese molybdate surface. As a consequence, these systems can have different acidities, and this is indeed demonstrated by  $\text{NH}_3$  TPD data (see below).

In order to see how the properties of the catalysts depend on the heat-treatment temperature, we recorded the lattice vibration spectra of the molybdates before and after they were heat-treated in air at various temperatures.

As the heat-treatment temperature is raised, the spectrum of manganese molybdate in the range examined changes insignificantly. A band at  $610\text{ cm}^{-1}$ , which was discussed above, appears in the spectrum of  $\text{MnMoO}_4$  deposited from an aqueous suspension. The spectra recorded between  $500$  and  $1100\text{ cm}^{-1}$  for the cobalt and nickel catalysts heat-treated in air at various temperatures are presented in Figs. 2a and 2b, respectively. For these molybdates, the intensities of

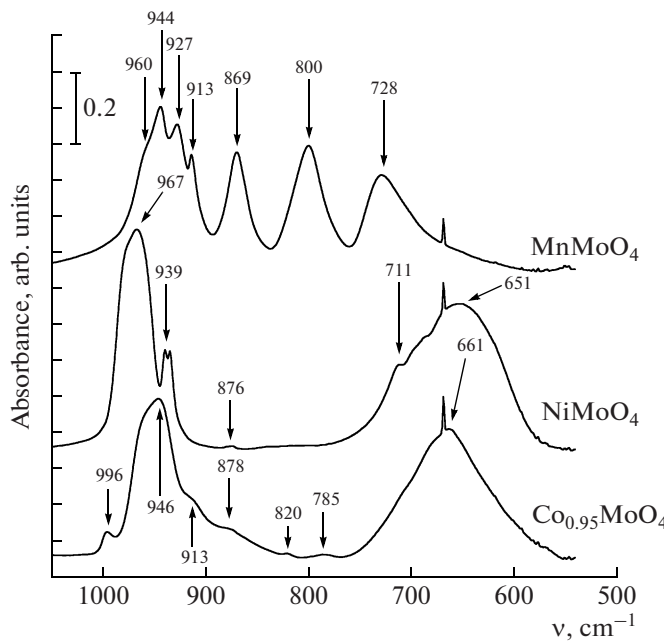


Fig. 1. IR absorption spectra of the air-dry catalysts  $\text{MnMoO}_4$ ,  $\text{NiMoO}_4$ , and  $\text{Co}_{0.95}\text{MoO}_4$ .

the absorption bands in the  $800$ – $900\text{ cm}^{-1}$  range increase as the heat-treatment temperature is raised. The spectrum of cobalt molybdate shows a marked strengthening of the absorption bands at  $842$ ,  $783$ , and  $706\text{ cm}^{-1}$  (Fig. 2a).

In the spectrum of untreated air-dry nickel molybdate (Fig. 1), no absorption bands occur near  $800\text{ cm}^{-1}$  and the absorption band at  $880\text{ cm}^{-1}$  is weak. After this sample is heat-treated above  $650^\circ\text{C}$ , its spectrum shows bands at  $881$ ,  $800$ , and  $715\text{ cm}^{-1}$  (Fig. 2b). The intensities of the first two bands increases significantly as the treatment temperature is raised to  $720^\circ\text{C}$ .

Under the assumption that the intensity of the absorption bands in the region examined correlates with the proportion of the molybdate with tetrahedrally coordinated molybdenum, it can be deduced that, during oxidative dehydrogenation at  $500$ – $550^\circ\text{C}$ , a considerable part of the cobalt molybdate turns into the  $\beta$ -phase and this can enhance the olefin selectivity. At the same time, the activation of nickel molybdate in air at  $550^\circ\text{C}$  does not cause any significant buildup of the  $\beta$ -phase. According to the literature [21–23],  $\beta$ - $\text{NiMoO}_4$  affords a much higher olefin selectivity in the oxidative dehydrogenation of lower paraffins than  $\alpha$ - $\text{NiMoO}_4$ . In the oxidative dehydrogenation of  $\alpha$ -butane on the  $\beta$ - and  $\alpha$ -phases, the olefin selectivity at  $12\%$  conversion is  $42$  and  $81\%$ , respectively; that is, the difference is almost  $40\%$  [21]. This is likely due to the fact that, under the reaction conditions, nickel molybdate contains only an insignificant proportion of tetrahedrally coordinated molybdenum. At the same time, we found that the olefin selectivities in the oxidative dehydrogenation of  $\beta$ -butane on the  $\alpha$ - and

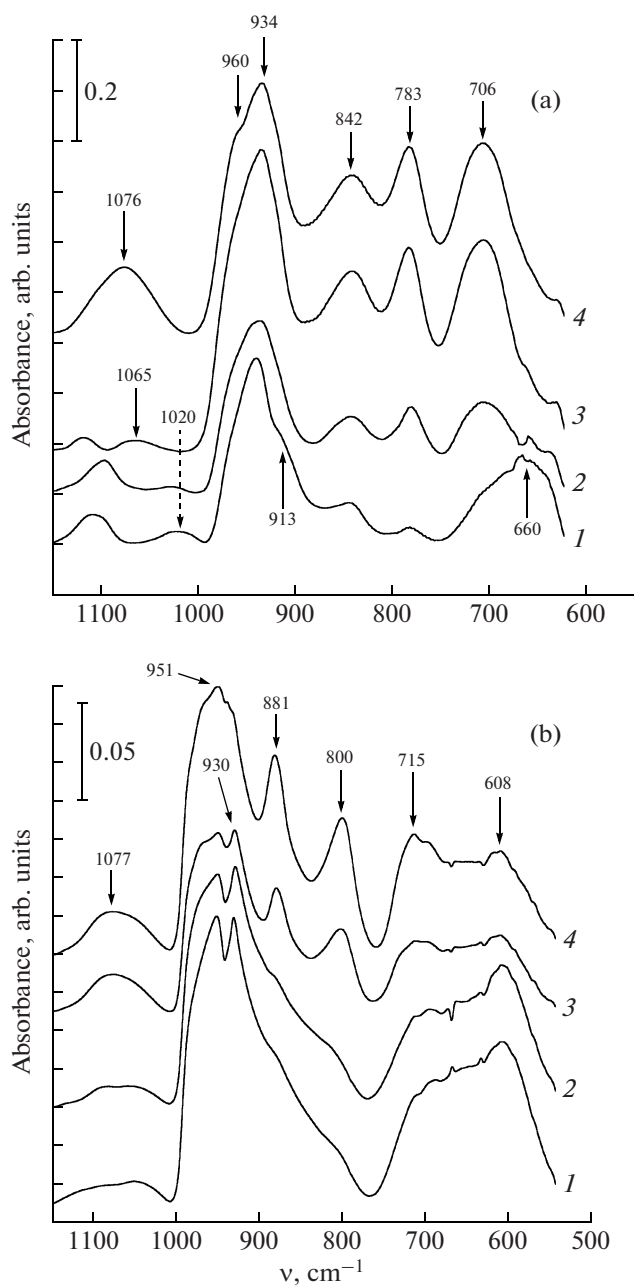


Fig. 2. IR absorption spectra in the lattice vibration region recorded for (a)  $\text{Co}_{0.95}\text{MoO}_4$  and (b)  $\text{NiMoO}_4$  after their heat treatment in air at (1) 150, (2) 550 (2 h), (3) 650 (30 min), and (4) 720°C (30 min).

$\beta$ -phases of cobalt molybdate differ by at most 10%, as distinct from what was observed for  $\text{NiMoO}_4$ . This is likely explained by the fact that a considerable part of the  $\alpha$ - $\text{CoMoO}_4$  turns into the  $\beta$ -phase at the reaction temperature.

#### Isobutene Adsorption

Isobutene adsorption was studied by recording the IR spectra of C–H bond vibrations in the 2500–

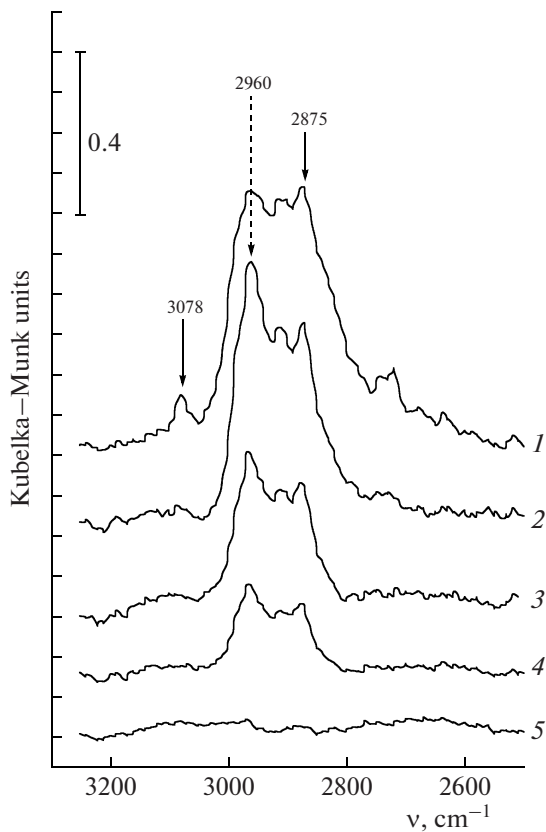


Fig. 3. IR spectra of  $\text{NiMoO}_4$  (1) after isobutene adsorption (20 Torr) at 20°C, (2) after pumping down to a residual pressure of  $10^{-3}$  atm at 20°C for 1 h, (3) after pumping at 100°C for 1 h, (4) after pumping at 200°C for 1 h, and (5) after pumping at 300°C for 1 h.

3100  $\text{cm}^{-1}$  range. The catalysts to be examined were calcined in air at 550°C for 2 h and were then pumped at 200°C for 1 h to a residual pressure of  $10^{-3}$  atm. Next, isobutene was admitted into the cell with the catalyst at 20°C and 20 Torr and the spectrum in the region of the characteristic C–H vibrations in adsorbed hydrocarbons was recorded at different desorption stages. By way of example, we present the spectra of  $\text{NiMoO}_4$  (Fig. 3). According to the literature [3, 19], the absorption band at 3078  $\text{cm}^{-1}$  is due to the  $\nu_{\text{as}}(\text{C–H})$  vibrations of the  $=\text{CH}_2$  group and the strongest band is due to the asymmetric vibrations of the C–H bond in the  $-\text{CH}_3$  group. This band occurs at 2960  $\text{cm}^{-1}$  in the spectrum of the cobalt catalyst, at 2958  $\text{cm}^{-1}$  in the spectrum of  $\text{NiMoO}_4$ , and at 2978  $\text{cm}^{-1}$  in the spectrum of  $\text{MnMoO}_4$ . The band near 2870  $\text{cm}^{-1}$  is due to the  $\nu_s(\text{C–H})$  vibrations in the methyl group.

Under the conditions of our IR spectroscopic experiment ( $<300^\circ\text{C}$ ), the observed spectral changes certainly arise from isobutene adsorption and desorption. A number of studies devoted to the oxidative dehydrogenation of  $\text{C}_2$  and  $\text{C}_3$  olefins and isobutane on molybdates (see, e.g., [1, 2, 24, 25]) demonstrated

that the partial and total oxidation of these hydrocarbons become noticeable above 400°C and their cracking begins above 500°C.

The results of our experiments suggest that the strength of the olefin–catalyst surface bond decreases in the order  $\alpha\text{-NiMoO}_4 > \beta\text{-Co}_{0.95}\text{MoO}_4 > \text{MnMoO}_4$ . The manganese molybdate surface desorbs the adsorbed olefin almost entirely at 100°C. Most of the isobutene adsorbed on the cobalt catalyst is desorbed between 100 and 200°C. As distinct from these catalysts, nickel molybdate retains appreciable amounts of the olefin above 200°C (Fig. 3).

#### Acidity of the Catalysts

The effect of the acidity of the molybdates on their catalytic properties in the oxidative dehydrogenation reaction was studied by ammonia TPD. The TPD profiles for these catalysts are presented in Fig. 4. The results of the deconvolution of these profiles and calculated amounts of ammonia desorbed from various sites of the catalysts are presented in the table. The largest amount of  $\text{NH}_3$  is desorbed from the acid sites of  $\alpha\text{-CoMoO}_4$  and  $\text{NiMoO}_4$ . The smallest amount of ammonia is desorbed from manganese molybdate, particularly at high temperatures.

Formally dividing the acid sites into weak (desorbing ammonia below 350°C) and strong (desorbing ammonia at 350°C and above), it is possible to reveal some regularities. The diagram presented in Fig. 5 demonstrates that it is the changes in the strong acidity of the molybdates (B) that correlate with the IR spectroscopic data for adsorbed isobutene. In addition, the acidity of the catalysts is correlated in a certain way with the isobutene selectivity (C) in the oxidative dehydrogenation of isobutane [1, 2], although this factor is not crucial to the process. The higher the concentration of strong acid sites, the longer the retention time of olefins on the catalyst surface and, accordingly, the larger the contribution from the side reactions—oxidation, cracking, and coking.

#### $\text{NH}_3$ TPD data for Co, Ni, and Mn molybdates

Catalyst	Amount of $\text{NH}_3$ desorbed at different temperatures, $\mu\text{mol/g}_{\text{Cat}}$					Total amount of ammonia desorbed, $\mu\text{mol/g}_{\text{Cat}}$
$\text{NiMoO}_4$	145°C	240°C	383°C	443°C	542°C	43.7
	12.7	7.0	6.6	7.4	9.9	
$\alpha\text{-Co}_{0.95}\text{MoO}_4$	147°C	227°C	311°C	403°C	489°C	33.3
	14.5	7.7	4.3	4.5	2.3	
$\beta\text{-Co}_{0.95}\text{MoO}_4$	131°C	205°C	288°C	388°C	460°C	9.6
	3.0	1.5	1.0	0.8	3.3	
$\text{MnMoO}_4$	142°C	194°C	260°C	361°C	—	6.6
	14.5	7.7	4.3	4.5	—	

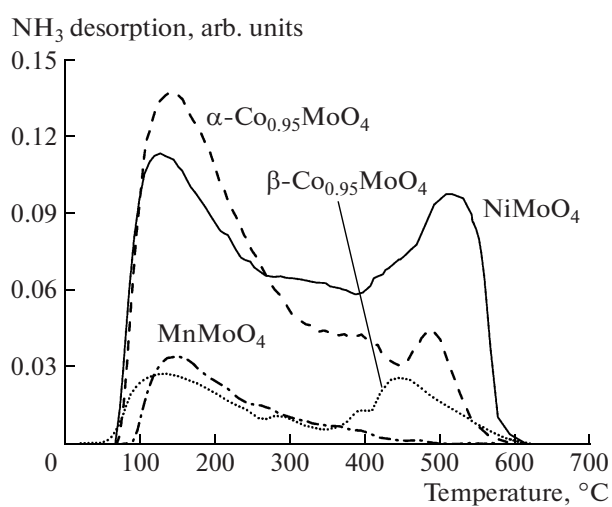
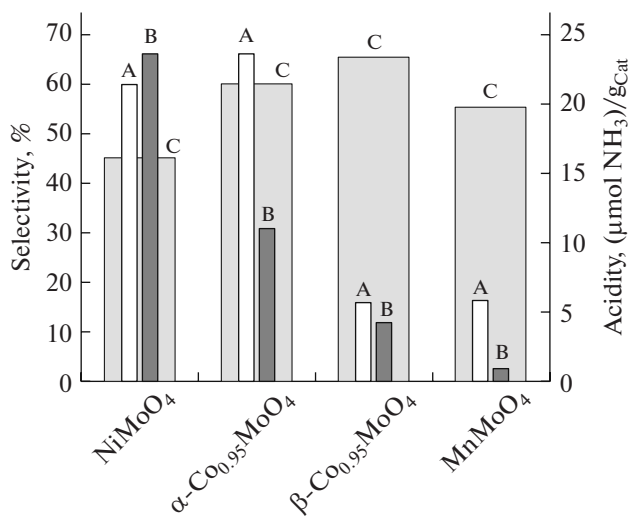


Fig. 4. Ammonia TPD profiles for Co, Ni, and Mn molybdates.

Having a low acidity and a low olefin adsorption capacity,  $\text{MnMoO}_4$  is highly active in the deep oxidation of hydrocarbons [2]. As a consequence, this catalyst cannot afford a high isobutene yield in the oxidative hydrogenation of isobutane.

Thus, the nature of the divalent ion and the coordination of molybdenum in the crystal lattice have a strong effect on the acid properties of the molybdates. The olefin adsorption properties of the molybdates can be determined both by the nature of the divalent ion and by the coordination of molybdenum in the lattice. Under the conditions of the oxidative dehydrogenation of isobutane, a considerable part of the molybdenum in  $\text{Co}_{0.95}\text{MoO}_4$  is tetrahedrally coordinated, while nickel molybdate retains the octahedral coordination of molybdenum, which favors the formation of stronger bonds with olefins.

This study confirms the conclusions drawn from our earlier investigation of the kinetics and mechanism of the oxidative dehydrogenation of isobutane [1, 2]. These conclusions pertain to the adsorption



**Fig. 5.** Correlation of (A) weak and (B) strong acidities of Co, Ni, and Mn molybdates with (C) their isobutene selectivity in the oxidative dehydrogenation of isobutane (8% conversion,  $T = 500^\circ\text{C}$ ).

properties of the molybdates with respect to the olefins involved in the process: the increase in the surface concentration of strong acid sites in the order  $\text{MnMoO}_4 > \beta\text{-Co}_{0.95}\text{MoO}_4 > \alpha\text{-NiMoO}_4$  correlates with the olefin adsorption strength. Thus, a low density of adsorption sites and weak olefin binding to these sites are necessary, but not sufficient, conditions for a catalyst to be efficient in the oxidative dehydrogenation of isobutane.

## REFERENCES

- Agafonov, Yu.A., Nekrasov, N.V., and Gaidai, N.A., *Kinet. Katal.*, 2001, vol. 42, no. 6, p. 899 [*Kinet. Catal.* (Engl. Transl.), vol. 42, no. 6, p. 821].
- Agafonov, Yu.A., Nekrasov, N.V., Gaidai, N.A., and Lapidus, A.L., *Kinet. Katal.*, 2007, vol. 48, no. 2, p. 271 [*Kinet. Catal.* (Engl. Transl.), vol. 48, no. 2, p. 255].
- Davydov, A.A., *Kinet. Katal.*, 1979, vol. 20, no. 6, p. 1506.
- Henrici-Olive, G. and Olive, S., *Coordination and Catalysis*, Weinheim: Chemie, 1977.
- Mazzocchia, C., Aboumrad, Ch., Diagne, C., Tempesti, E., Herrmann, J.M., and Thomas, G., *Catal. Lett.*, 1991, vol. 10, nos. 3–4, p. 181.
- Madeira, L.M., Martin-Aranda, R.M., Maldonado-Hodar, F.J., Fierro, J.L.G., and Portela, M.F., *J. Catal.*, 1997, vol. 169, no. 2, p. 469.
- Tret'yakov, Yu.D., *Tverdofaznye reaktsii* (Solid-Phase Reactions), Moscow: Khimiya, 1978.
- Abrahams, S.C. and Reddy, J.M., *J. Chem. Phys.*, 1965, vol. 43, no. 7, p. 2533.
- Zakharov, I.I., Popova, G.Y., and Andrushkevich, T.V., *React. Kinet. Catal. Lett.*, 1982, vol. 19, nos. 3–4, p. 367.
- Abello, M.C., Gomez, M.F., and Cadus, L.E., *Catal. Lett.*, 1998, vol. 53, nos. 3–4, p. 185.
- Abello, M.C., Gomez, M.F., and Ferretti, O., *Appl. Catal., A*, 2001, vol. 207, nos. 1–2, p. 421.
- Mazzocchia, C., Renzo, F., Aboumrad, C., and Thomas, G., *Solid State Ionics*, 1989, vol. 32, no. 2, p. 228.
- Cadus, L.E., Abello, M.C., Gomez, M.F., and Rivarola, J.B., *Ind. Eng. Chem. Res.*, 1996, vol. 35, no. 1, p. 14.
- Davydov, A.A., *React. Kinet. Catal. Lett.*, 1982, vol. 19, nos. 3–4, p. 377.
- Dury, F., Centeno, M.A., Gaigneaux, E.M., and Ruiz, P., *Appl. Catal., A*, 2003, vol. 247, no. 2, p. 231.
- Abrahams, S.C. and Reddy, J.M., *J. Chem. Phys.*, 1965, vol. 43, no. 7, p. 2533.
- Liu, Y., Wang, J., Zhou, G., Xian, Mo., Bi, Y., and Zhen, K., *React. Kinet. Catal. Lett.*, 2001, vol. 73, no. 2, p. 199.
- Yoon, Y.S., Suzuki, K., Hayakawa, T., Shishido, T., and Takehira, K., *Catal. Lett.*, 1999, vol. 59, nos. 2–4, p. 165.
- Davydov, A.A., *IK-Spektroskopiya v khimii poverkhnosti okislov* (IR Spectroscopy Applied to the Chemistry of Oxide Surfaces), Novosibirsk: Nauka, 1984.
- Meullemeestre, J. and Penigault, F., *Bull. Soc. Chim. Fr.*, 1975, vol. 354, nos. 9–10, p. 1925.
- Portela, M.F., Aranda, M.R., Madeira, M., Oliveira, M., Freire, F., Anouchinsky, R., Kaddouri, A., and Mazzocchia, C., *Chem. Commun.*, 1996, vol. 6, p. 501.
- Tempesti, E., Kaddouri, A., and Mazzocchia, C., *Appl. Catal., A*, 1998, vol. 166, no. 2, p. L259.
- Kaddouri, A., Mazzocchia, C., and Tempesti, E., *Appl. Catal., A*, 1998, vol. 169, no. 1, p. L3.
- Madeira, L.M., Portela, M.F., Kaddouri, A., Mazzocchia, C., and Anouchinsky, R., *Catal. Today*, 1998, vol. 40, no. 2, p. 229.
- Yoon, Y.S., Ueda, W., and Moro-oka, Y., *Top. Catal.*, 1996, vol. 3, nos. 3–4, p. 265.